LA-UR-12-25115
Approved for public release; distribution is unlimited.

Title: Structural Characterization and Thermochemical Measurements of Ba/Ti-Substituted Pollucites for Radioactive Cs Immobilization

Author(s): Xu, Hongwu
Chavez, Manuel E.
Mitchell, Jeremy N.

Intended for: Report

Structural Characterization and Thermochemical Measurements of Ba/Ti-Substituted Pollucites for Radioactive Cs Immobilization

H. Xu, M.E. Chavez and J.N. Mitchell

EES and MST Divisions, Los Alamos National Laboratory, NM

Introduction

Pollucite, $CsAlSi_2O_6$, has a three-dimensional framework structure composed of corner-sharing $[SiO_4]$ and $[AlO_4]$ tetrahedra with Cs^+ cations occupying the cavities. Substituting Ti^{4+} for Al^{3+} over the tetrahedral sites, accompanied by incorporation of extra O^{2-} into the structure to achieve its charge neutrality, produces a series of substituted pollucites with the general formula $CsTi_xAl_{1-x}Si_2O_{6+0.5x}$ (x = 0 to 1) (Balmer et al. 1997, Xu et al. 2001, 2002). This group of materials is of considerable interest as potential hosts for radioactive Cs. The end-member pollucite has long been proposed for Cs immobilization because of its relatively high resistance to alteration under hydrothermal conditions. The discovery of microporous silicotitanate ion exchangers (e.g., Anderson et al. 1995) has spurred interest in the crystalline silicotitanate (CST) waste form in which Ti-substituted pollucites are probable Cs-host phases. Specifically, some CST ion exchangers have been found to possess high selectivity for Cs^+ over other alkali ions (such as Na^+), and, thus, they can be used for separation of radioactive ^{137}Cs from aqueous nuclear wastes. The Cs-loaded CST phases can then be heat-treated *in situ* to produce a stable and refractory ceramic waste form. In particular, as a potential host for Cs in the proposed waste form, the Ti-substituted end member, $CsTiSi_2O_{6.5}$, has been found to have Cs leach rates at least comparable to those of aluminosilicate pollucite.

^{137}Cs is a fission product of uranium and occurs as a major heat-generating radionuclide in nuclear wastes. It transforms to ^{137}Ba through beta decay with a half-life of about 30 years. Therefore, to utilize $CsTiSi_2O_{6.5}$ and related phases as long-term hosts for ^{137}Cs, one must understand the effects of the $^{137}Cs \rightarrow {}^{137}Ba$ decay on the structures and stability of Ti-substituted pollucites. However, because of the long time required for the decay to occur (30-year half-life), it is not practicable to perform the decay experiments directly within a reasonable period of time. Instead, one may synthesize Ba/Ti-substituted

pollucites with various Ba/Cs ratios and determine their crystal structures and thermodynamic properties at various conditions. Systematic studies of these pollucites will shed import light on the effects that the $^{137}Cs \rightarrow {}^{137}Ba$ decay may exert on the long-term stability of pollucite phases.

Samples

Garino et al. (2009) synthesized two series of Ba-substituted $CsTiSi_2O_{6.5}$ materials, $Cs_xBa_{(1-x)/2}TiSi_2O_{6.5}$ and $Cs_xBa_{1-x}TiSi_2O_{7-0.5x}$, with the pollucite structure. First, a precursor with the targeted composition was prepared. Second, the precursor was mixed with seed crystals of $CsTiSi_2O_{6.5}$, and the mixture was then heat-treated to induce crystallization of the desired phase. In this work, eight samples with the compositions $Cs_xBa_{(1-x)/2}TiSi_2O_{6.5}$ and $Cs_xBa_{1-x}TiSi_2O_{7-0.5x}$, x = 0.95, 0.9, 0.85 and 0.7, were synthesized using the above method (by T. Garino and T. Nenoff at Sandia National Laboratories).

Synchrotron X-ray diffraction

To characterize the purity and structures of the above samples, high-resolution powder synchrotron X-ray diffraction (XRD) data were collected at beamline 11-BM at the Advanced Photon Source (APS), Argonne National Laboratory, using a wavelength of 0.413915 Å. Discrete detectors covering an angular range from -6 to 16º 2θ were scanned over a 34º 2θ range, with data points collected every 0.001º 2θ at a scan speed of 0.01º/s (Lee et al. 2008).

Our analyses of the obtained synchrotron data indicate that the $Cs_xBa_{(1-x)/2}TiSi_2O_{6.5}$ samples with x = 0.9 and 0.7 consist of the Ba/Ti-substituted pollucites. However, other six samples contain small amounts of fresnoite ($Ba_2TiSi_2O_6$), and further, the $Cs_xBa_{(1-x)/2}TiSi_2O_{6.5}$ and $Cs_xBa_{1-x}TiSi_2O_{7-0.5x}$ samples with x = 0.95 and 0.85 contain some other unknown impurities as well. Thus, for later structural analyses, we focus on the two pure samples only. For thermochemical measurements, it is also ideal to have pure samples, but well-characterized samples containing a small amount of minor phase should also be useful. Hence, we have conducted high-temperature calorimetric experiments on four $Cs_xBa_{(1-x)/2}TiSi_2O_{6.5}$ and $Cs_xBa_{1-x}TiSi_2O_{7-0.5x}$ samples with x = 0.9 and 0.7.

The synchrotron data for $Cs_xBa_{(1-x)/2}TiSi_2O_{6.5}$ phases with $x = 0.9$ and 0.7 were analyzed using the Rietveld method with the General Structure Analysis System (GSAS) program of Larson and Von Dreele (2000). The starting structural parameters were taken from the study of the prototype phase $CsTiSi_2O_{6.5}$ by Balmer et al. (1997). The final fitted XRD patterns are plotted in Fig. 1. The refinement agreement parameters, unit-cell parameters, atomic coordinates, and atomic displacement parameters are presented in Fig. 1 and Tables 1 and 2.

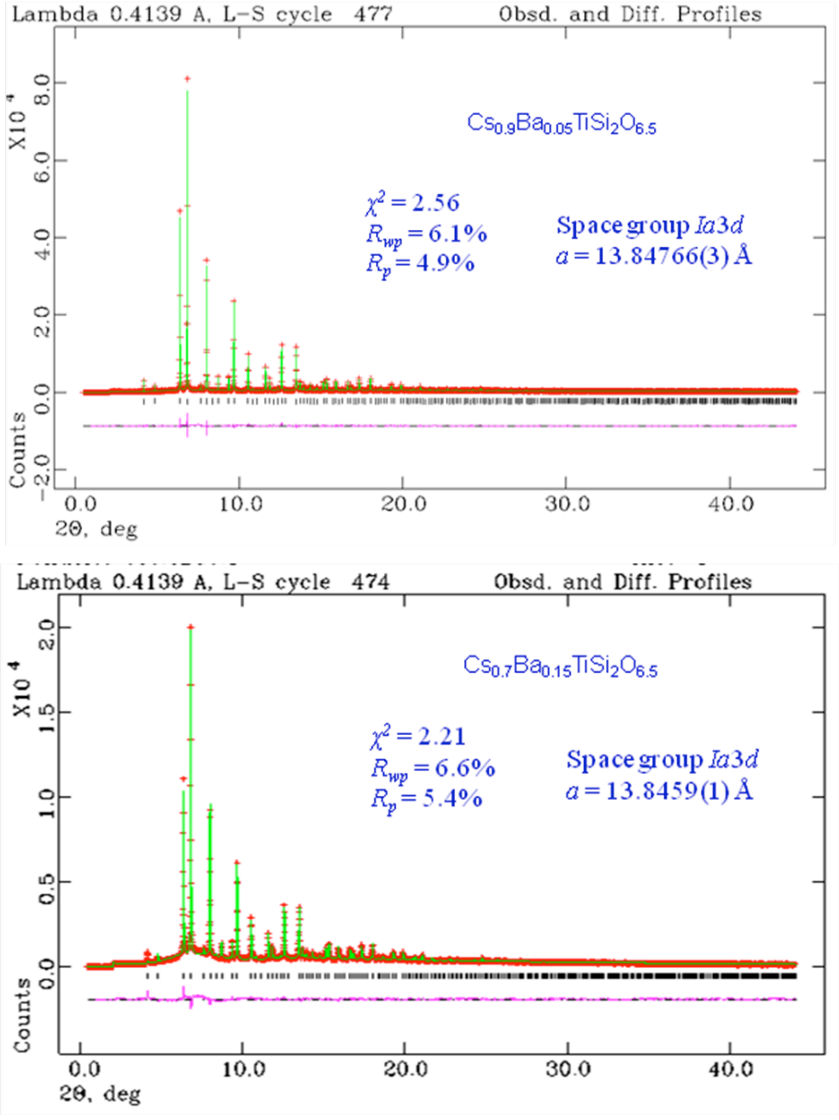

Figure 1. Fitted synchrotron XRD patterns of $Cs_xBa_{(1-x)/2}TiSi_2O_{6.5}$ phases with $x = 0.9$ (upper) and $x = 0.7$ (lower). Data are shown as plus signs, and the solid curve is the best fit to the data. Tick marks below the pattern show the positions of allowed reflections,

and the lower curve represents the difference between the observed and calculated profiles.

Table 1. Atomic coordinates and atomic displacement parameters of $Cs_{0.9}Ba_{0.05}TiSi_2O_{6.5}$

atom	*x*	*y*	*z*	U_{iso} (100/Å)
Cs/Ba	0.125	0.125	0.125	4.88(1)
Si/Ti	0.66621(5)	0.58379(5)	0.125	4.81(3)
O	0.10554(9)	0.13454(9)	0.7164(1)	8.07(5)

Table 2. Atomic coordinates and atomic displacement parameters of $Cs_{0.7}Ba_{0.15}TiSi_2O_{6.5}$

atom	*x*	*y*	*z*	U_{iso} (100/Å)
Cs/Ba	0.125	0.125	0.125	5.01(2)
Si/Ti	0.66707(9)	0.58293(9)	0.125	7.84(5)
O	0.1043(2)	0.1328(2)	0.7153(2)	10.3(1)

As shown in Fig. 1, the unit-cell parameter *a* of $Cs_{0.7}Ba_{0.15}TiSi_2O_{6.5}$ (13.8459 Å) is smaller than that of $Cs_{0.9}Ba_{0.05}TiSi_2O_{6.5}$ (13.8477 Å), which, in turn, is smaller than the *a* value of $CsTiSi_2O_{6.5}$ (13.8494 Å) (Xu et al. 2002). This trend is possibly because the amount of Ba^{2+} is only half that of the substituted Cs^+ plus Ba^{2+} is smaller than Cs^+, thereby resulting in the structural contraction. This, however, may not be the case for the $Cs_xBa_{1-x}TiSi_2O_{7-0.5x}$ series, as the replacement of Cs^+ by the same amount of the smaller Ba^{2+} is accompanied by incorporation of additional O^{2-}, where their effects on the titanosilicate framework are probably opposite. Moreover, in the $Cs_xBa_{1-x}TiSi_2O_{7-0.5x}$ counterpart samples with $x = 0.9$ and 0.7, fresnoite ($Ba_2TiSi_2O_6$) is present, and, further, its amount increases with increasing Ba content (decreasing *x*). This behavior suggests that the $Cs^+ \rightarrow Ba^{2+} + 0.5O^{2-}$ substitution mechanism may be operating at up to a very limited extent, i.e., at least smaller than 10% ($x > 0.9$). To obtain a more decisive

conclusion, additional characterization of these impure samples (including the four samples with $x = 0.95$ and 0.85) by other techniques such as transmission electron microscopy and electron microprobe analysis would be needed.

Thermochemical measurements

High-temperature calorimetric measurements were performed using a Setaram AlexSys-800 microcalorimeter operating at about 973 K. This calorimeter follows the Tian-Calvet design and consists of twinned sample chambers that are each surrounded by a Pt-PtRh thermopile connecting to a massive metallic block maintained at a constant temperature. The twined design increases measurement productivity and minimizes the effects of small drifts in temperature. Three types of experiments can be performed with this kind of calorimeter: 1) transposed temperature drop calorimetry, 2) solution calorimetry, and 3) drop-solution calorimetry. In 1), a sample is dropped from room temperature into the hot but solventless calorimeter, and the heat content (HC) is measured. In 2), the sample is first equilibrated in the hot calorimeter and is then dropped into the solvent, where the enthalpy of solution, ΔH_s, is measured. In 3), the sample is dropped from room temperature into solvent, and the measured heat is the sum of the heat content (HC) and the enthalpy of solution (ΔH_s), which is called the enthalpy of drop solution (ΔH_{ds}).

Prior to each set of experiments, the calorimeter typically needs to be calibrated against the known heat content of alumina (α-Al_2O_3) by transposed temperature drop calorimetry (or on a monthly basis). Several alumina pellets weighing ~5 mg were dropped from room temperature into each sample chamber of the calorimeter at about 973 K. The calibration factors of both sample chambers were then computed as the ratios of the known heat contents of the alumina pellets (J/g) to their measured heats ($\mu V \cdot min/g$) from the calorimeter.

Transposed temperature drop calorimetric measurements were conducted on four $Cs_xBa_{(1-x)/2}TiSi_2O_{6.5}$ and $Cs_xBa_{1-x}TiSi_2O_{7-0.5x}$ samples with $x = 0.9$ and 0.7. As described earlier, the other four samples contain unknown impurities and thus were not measured. Like the alumina calibration runs, these experiments involved dropping a sample pellet (~5 mg) from room temperature into the hot calorimeter, without the presence of a

solvent. A pair of representative plots of heat flow versus time for $Cs_{0.9}Ba_{0.05}TiSi_2O_{6.5}$ is shown in Fig. 2. The area under each curve is proportional to the involved heat effect, which corresponds to the heat content, HC = $H_{973} - H_{298}$, of the sample. Table 3 lists the obtained heat contents of the four samples. As is shown, these values are essentially the same within the experimental uncertainties, suggesting that the substitutions $Cs^+ \rightarrow 0.5Ba^{2+}$ (in the $Cs_xBa_{(1-x)/2}TiSi_2O_{6.5}$ series) and $Cs^+ \rightarrow Ba^{2+} + 0.5O^{2-}$ (in the $Cs_xBa_{1-x}TiSi_2O_{7-0.5x}$ series) have small effect on the heat contents of Ba/Ti-substituted pollucites. Note that the two $Cs_xBa_{1-x}TiSi_2O_{7-0.5x}$ samples (x = 0.9 and 0.7) contain minor amounts of fresnoite, and thus their heat contents need to be corrected by accounting for the heat content of fresnoite. Nevertheless, since the amounts of fresnoite are small, the corrections are expected to small as well.

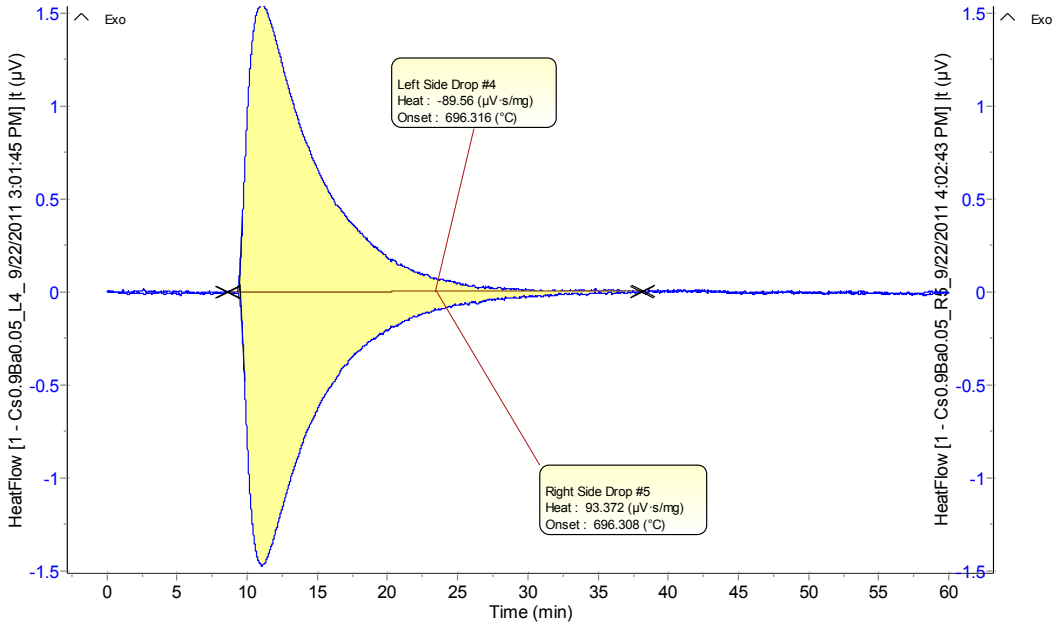

Figure 2. Representative plots of heat flow (µV) versus time (minute) of $Cs_{0.9}Ba_{0.05}TiSi_2O_{6.5}$ pollucite. The upper and lower curves are from the drops into the left and right sample chambers, respectively.

Table 3. Heat contents of $Cs_xBa_{(1-x)/2}TiSi_2O_{6.5}$ and $Cs_xBa_{1-x}TiSi_2O_{7-0.5x}$ samples (x = 0.9 and 0.7)

composition	$H_{973} - H_{298}$ (kJ/mol)*
$Cs_{0.9}Ba_{0.05}TiSi_2O_{6.5}$	157.2 ± 2.5 (6)
$Cs_{0.7}Ba_{0.15}TiSi_2O_{6.5}$	161.0 ± 2.7 (6)
$Cs_{0.9}Ba_{0.10}TiSi_2O_{6.55}$	160.7 ± 5.6 (5)
$Cs_{0.7}Ba_{0.30}TiSi_2O_{6.65}$	164.7 ± 4.5 (4)

*Uncertainty is two standard deviation of the mean; value in parentheses is the number of experiments.

Drop-solution calorimetric experiments of the same four $Cs_xBa_{(1-x)/2}TiSi_2O_{6.5}$ and $Cs_xBa_{1-x}TiSi_2O_{7-0.5x}$ samples (x = 0.9 and 0.7) were conducted using molten lead borate ($2PbO{\cdot}B_2O_3$) solvent at about 973 K. The obtained heats of drop-solution (ΔH_{ds}) are listed in Table 4. Note that the two $Cs_xBa_{1-x}TiSi_2O_{7-0.5x}$ samples (x = 0.9 and 0.7) contain minor amounts of fresnoite, and their heat effects are ignored in these ΔH_{ds} values (as well as the heat contents, described earlier). From these data and the measured heat contents, ($H_{973} - H_{298}$) (Table 3), the heats of solution (ΔH_s) can be computed as $\Delta H_s = \Delta H_{ds} - (H_{974} - H_{298})$ (Table 4). In contrast to the similarity in heat content for the four compositions, both ΔH_{ds} and ΔH_s enthalpies become less endothermic with increasing Ba content or decreasing Cs content. This behavior implies an endothermic enthalpy of the Cs → Ba substitution in the Ti-substituted pollucite structure.

Using thermodynamic parameters of the constituent oxides (Cs_2O, BaO, TiO_2, and SiO_2) (Table 5) and the measured drop-solution data (Table 4), we calculated the standard molar enthalpies of formation of $Cs_xBa_{(1-x)/2}TiSi_2O_{6.5}$ (x = 0.9 and 0.7) from the oxides ($\Delta H^o_{f,ox}$) and the enthalpies of formation from the elements ($\Delta H^o_{f,el}$) via thermochemical cycles listed in Table 6. Similarly, the formation enthalpies $\Delta H^o_{f,ox}$ and $\Delta H^o_{f,el}$ of $Cs_xBa_{1-x}TiSi_2O_{7-0.5x}$ phases can be derived by using appropriate reaction cycles. The enthalpies of formation thus obtained are presented in Table 7. As shown in Table 7, the enthalpies

of formation from the constituent oxides ($\Delta H^{o}_{f,ox}$) of the two $x = 0.9$ phases are more exothermic than those of the two $x = 0.7$ phases, regardless of the specific charge-coupled substitution mechanism. In other words, with increasing Ba content and decreasing Cs content, the thermodynamic stability of these Ba/Ti-substituted pollucites appears to decrease with respective to their component oxides. Hence, from the energetic viewpoint, the Cs → Ba substitution mechanism in these phases may be operating at up to a certain extent. These thermochemical measurements, together with our synchrotron XRD results, thus provide important insights into the effects of the $^{137}Cs \rightarrow {}^{137}Ba$ decay on the phase stability of these wasteform materials.

Table 4. Heats of drop solution (ΔH_{ds}) and heats of solution (ΔH_s) of $Cs_xBa_{(1-x)/2}TiSi_2O_{6.5}$ and $Cs_xBa_{1-x}TiSi_2O_{7-0.5x}$ samples ($x = 0.9$ and 0.7) in lead borate solvent at 973 K

composition	ΔH_{ds} (kJ/mol)*	ΔH_s (kJ/mol)
$Cs_{0.9}Ba_{0.05}TiSi_2O_{6.5}$	193.4 ± 4.2 (6)	36.2 ± 4.9
$Cs_{0.7}Ba_{0.15}TiSi_2O_{6.5}$	168.4 ± 4.9 (3)	7.4 ± 5.6
$Cs_{0.9}Ba_{0.10}TiSi_2O_{6.55}$	201.5 ± 3.0 (6)	40.8 ± 6.3
$Cs_{0.7}Ba_{0.30}TiSi_2O_{6.65}$	161.6 ± 5.1 (5)	-3.1 ± 6.8

*Uncertainty is two standard deviation of the mean; value in parentheses is the number of experiments.

Table 5. Heats of drop solution in lead borate at 973 K (ΔH_{ds}) and enthalpies of formation from the elements ($\Delta H^{o}_{f,el}$) at 298 K of related component oxides

Oxide	ΔH_{ds} (kJ/mol)	$\Delta H^{o}_{f,el}$ (kJ/mol)
Cs_2O	-183.3 ± 1.4[1)]	-346.0 ± 1.2[4)]
BaO	-91.5 ± 1.9[2)]	-548.1 ± 2.1[4)]
TiO_2	55.4 ± 1.2[3)]	-944.0 ± 0.8[4)]
SiO_2	39.1 ± 0.3[2)]	-910.7 ± 1.0[4)]

1) Xu et al. (2000); 2) Kiseleva et al. (1996); 3) Putnam et al. (1999); 4) Robie and Hemingway (1995)

Table 6. Thermochemical cycles used for calculation of the enthalpies of formation of $Cs_xBa_{(1-x)/2}TiSi_2O_{6.5}$ pollucites

---

Enthalpy of formation of $Cs_xBa_{(1-x)/2}TiSi_2O_{6.5}$ from the oxides at 298 K ($\Delta H^o_{f,ox}$)

$Cs_xBa_{(1-x)/2}TiSi_2O_{6.5}$(s, 298 K) → xCsO(soln, 973 K)+ (1-x)/2BaO(soln, 973 K) + TiO_2(soln, 973 K) + 2SiO_2(soln, 973 K) ΔH_{ds}

xCsO(s, 298 K) → xCsO(soln, 973 K) ΔH_1

(1-x)/2BaO(s, 298 K) → (1-x)/2BaO(soln, 973 K) ΔH_2

TiO_2(s, 298 K) → TiO_2(soln, 973 K) ΔH_3

2SiO_2(s, 298 K) → 2SiO_2(soln, 973 K) ΔH_4

xCsO(s, 298 K)+ (1-x)/2BaO(s, 298 K) + TiO_2(s, 298 K) + 2SiO_2(s, 298 K) → $Cs_xBa_{(1-x)/2}TiSi_2O_{6.5}$(s, 298 K) $\Delta H^0_{f,ox} = \Sigma\Delta H_i$ (i = 1-4) – ΔH_{ds}

Enthalpy of formation of $Cs_xBa_{(1-x)/2}TiSi_2O_{6.5}$ from the elements at 298 K ($\Delta H^o_{f,el}$)

xCsO(s, 298 K)+ (1-x)/2BaO(s, 298 K) + TiO_2(s, 298 K) + 2SiO_2(s, 298 K) → $Cs_xBa_{(1-x)/2}TiSi_2O_{6.5}$(s, 298 K) $\Delta H^0_{f,ox}$

xCs(s, 298 K) + x/2O_2(g, 298 K) → xCsO(s, 298 K) ΔH_5

(1-x)/2Ba(s, 298 K) + (1-x)/4O_2(s, 298 K) → (1-x)/2BaO(s, 298 K) ΔH_6

Ti(s, 298K) + O_2(g, 298 K) → TiO_2(s, 298 K) ΔH_7

2Si(s, 298K) + O_2(g, 298 K) → 2SiO_2(s, 298 K) ΔH_8

xCs(s, 298 K)+ (1-x)/2Ba(s, 298 K) + Ti(s, 298 K) + 2Si(s, 298 K) + 3.25O_2(g, 298 K) → $Cs_xBa_{(1-x)/2}TiSi_2O_{6.5}$(s, 298 K) $\Delta H^0_{f,el} = \Delta H^0_{f,ox} + \Sigma\Delta H_i$ (i = 5-8)

Table 7. Enthalpies of formation of $Cs_xBa_{(1-x)/2}TiSi_2O_{6.5}$ and $Cs_xBa_{1-x}TiSi_2O_{7-0.5x}$ (x = 0.9 and 0.7) from the oxides ($\Delta H^o_{f,ox}$) and elements ($\Delta H^o_{f,el}$) at 298 K

composition	$\Delta H^o_{f,ox}$ (kJ/mol)	$\Delta H^o_{f,el}$ (kJ/mol)
$Cs_{0.9}Ba_{0.05}TiSi_2O_{6.5}$	-146.9 ± 4.5	-3095.4 ± 5.0
$Cs_{0.7}Ba_{0.15}TiSi_2O_{6.5}$	-112.7 ± 5.1	-3081.4 ± 5.5
$Cs_{0.9}Ba_{0.10}TiSi_2O_{6.55}$	-159.5 ± 3.3	-3135.4 ± 4.0
$Cs_{0.7}Ba_{0.30}TiSi_2O_{6.65}$	-119.6 ± 5.3	-3170.5 ± 5.8

References

Anderson, M.W. , Terasaki, O., Ohsuna, T. , Malley, P.J.O., Philippou, A. , MacKay, S.P., Ferreira, A., Rocha, J., and Lidin, S., *Philos. Mag. B, 71,* 831-841 (1995).

Balmer, M.L., Huang, Q., Wong-Ng, W., Roth, R.S. and Santoro, A., *J. Solid State Chem*., 130**,** 97–102 (1997).

Garino, T.J., Nenoff, T.M., Park, T.-J. and Navrotsky, A., *J. Am. Ceram. Soc.,* 92, 2144-2146 (2009).

Kiseleva, I., Navrotsky, A., Belitsky, I.A. and Fursenko, B.A., *Am. Mineral.*, 81, 658-667 (1996).

Larson, A.C. and Von Dreele, R.B. (2000) GSAS, General Structure Analysis System. Los Alamos National Laboratory, New Mexico.

Lee, P. L., Shu, D., Ramanathan, M., Preissner, C., Wang, J., Beno, M. A., Von Dreele, R. B., Lynn Ribaud, Kurtz, C., Antao, S. M., Jiao, X., and Toby, B. H., *J. Synchrotron Radiation 15*, 427-432 (2008).

Putnam, R.L., Navrotsky, A., Woodfield, B.F., Boerio-Goates, J. and Shapiro, J.L., *Chem. Thermodyn*., 31, 229-243 (1999).

Robie, R.A. and Hemingway, B.S. "Thermodynamic Properties of Minerals and Related Substances at 298.15 K and 1 Bar (105 Pascals) Pressure and Higher Temperatures," U.S. Geol. Survey Bull., 2131 (1995).

Xu, H., Navrotsky, A., Nyman, M.D. and Nenoff, T.M., *J. Mater. Chem*., *15*, 815-823 (2000).

Xu, H., Navrotsky, A., Balmer, M.L., Su, Y. and Bitten, E.R., *J. Am. Ceram. Soc.*, 84**,** 555-560 (2001).

Xu, H., Navrotsky, A., Balmer, M.L. and Su, Y., *J. Am. Ceram. Soc., 85*, 1235-1242 (2002).